

A reliable, compact, and low-cost Michelson wavemeter for laser wavelength measurement

P. J. Fox, R. E. Scholten, and M. R. Walkiewicz
School of Physics, University of Melbourne, Parkville Victoria 3052, Australia

R. E. Drullinger
Time and Frequency Division, National Institute of Standards and Technology, Boulder, Colorado 80303

(Received 14 September 1998; accepted 12 November 1998)

We describe the construction and operation of a simple, compact, and cost effective Michelson wavemeter with picometer accuracy. The low cost of the device means that it can form the basis of an undergraduate laboratory experiment, yet it is sufficiently reliable and accurate that it has become an important tool in our research laboratory, where it is regularly used to tune lasers to atomic transitions. The usefulness and accuracy of the wavemeter is demonstrated by tuning two separate extended cavity diode lasers to achieve two-step excitation of the Rb 5^2D state, observed by detecting 420 nm blue fluorescence from the $5^2D \rightarrow 6^2P \rightarrow 5^2S$ decay path. © 1999 American Association of Physics Teachers.

I. INTRODUCTION

Many experiments in atomic physics require tunable lasers, and with the introduction of low-cost tunable diode lasers,¹ such experiments have become feasible for undergraduate laboratories. However, these devices must first be tuned to the atomic transition of interest, requiring determination of the laser wavelength to within a Doppler-broadened linewidth, typically a few parts in 10^6 .

This can be achieved using various devices, such as a very high resolution spectrometer, a Fizeau or Fabry-Perot interferometer,^{2,3} or a Michelson wavemeter.^{4,5} Since their invention, traveling Michelson wavemeters have become a fundamental tool in most laser laboratories, where they provide an accurate and convenient method for measuring the wavelength of tunable lasers, reaching accuracies of order 10^{-9} to 10^{-11} .^{3,6,7}

Unfortunately, commercial wavemeters are often too expensive for undergraduate laboratories, and previously published wavemeter designs have focused on increasing accuracy beyond that required. We present a design which aims to reduce the cost, size, and complexity, yet retains accuracy sufficient for many atomic physics experiments.

The essential concept behind this type of wavemeter is simple: a Michelson interferometer is arranged to simultaneously detect interference fringes from two overlapping and copropagating laser beams, one of which has a known wavelength. The relative lengths of the interferometer arms are varied while interference fringes of both the known and unknown lasers are counted. The ratio of the two fringe counts gives the ratio of the wavelengths. Several mechanisms, such as a simple dc motor system based on a toy train,⁸ have been used to vary the interferometer path length. Greater accuracy and reliability have been obtained by using air tracks⁵ and roller bearing tracks.⁹ Improvements to the resolution have been achieved by increasing the number of fringes counted, either by lengthening the track significantly, folding the optical path again, or using fractional fringe counting or fringe multiplication.^{9,10}

The wavemeter described here is a compact version of the Hall and Lee design,⁴ with a simple, inexpensive air bearing. Air bearing technology was first adapted to wavemeter applications in this fashion by Drullinger in the 1970s, enabling

simple wavemeters with precision reaching one part in 10^9 .¹¹ The concept has since spread by word of mouth and been used successfully in wavemeters built in many research laboratories around the world. We use this idea in its simplest form and obtain highly repeatable measurements with a resolution of 1 pm and a relative accuracy of 3.8×10^{-6} . This is sufficient to tune a laser to a typical Doppler-broadened atomic resonance, yet the wavemeter can be constructed quickly from low-cost components.

We provide full details of the wavemeter, including technical drawings for the mechanical components and the electronics for the photodiode detectors and counting system. The wavemeter forms an ideal basis for an undergraduate laboratory project in optical interferometry, lasers, and atomic physics, introducing students to some of the principles of interferometry and measurement in a remarkably rewarding and satisfying project.

II. DESIGN AND OPERATIONAL PRINCIPLE

The principle behind the wavemeter is straightforward and described in detail elsewhere (Refs. 4 and 5), so only a brief review will be presented. Consider a simple Michelson interferometer, composed of two mirrors and a beamsplitter (Fig. 1). As mirror M1 is moved, the path difference between the two arms changes, resulting in changes in the interference pattern. The number of fringes counted as the mirror is moved distance d is $N_R = 2d/\lambda_R$, where λ_R is the wavelength of the reference laser. For a different (unknown) laser, at some wavelength λ_U , $N_U = 2d/\lambda_U$ fringes would be counted. If both lasers propagate through the interferometer simultaneously, then the distance moved by the mirror must be the same for each, giving

$$\lambda_U = \frac{N_R}{N_U} \lambda_R. \quad (1)$$

Provided that the wavelength of the first laser is well defined, the ratio of fringes counted gives the wavelength of the second laser.

Resolution of 1 in 10^6 is achieved if one million fringes are counted, which, for a 632.8 nm HeNe laser, means that the mirror in the Michelson interferometer must be moved

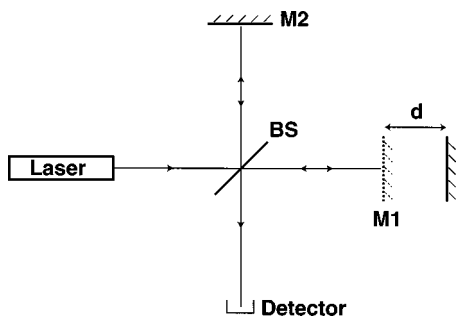


Fig. 1. Basic layout of a Michelson interferometer.

about 30 cm. This can be halved by using an arrangement whereby the mirrors in both arms of the interferometer are moved simultaneously, as shown in our configuration (Fig. 2). This arrangement is similar to that used previously,⁴ modified to reduce its size while maintaining ease of alignment. The entire wavemeter, including the HeNe reference laser, can be comfortably assembled on an aluminum plate 300 mm × 150 mm.

A HeNe laser is used as the reference since it is low in cost and has a well-defined wavelength. The plane mirrors are replaced with cornercubes, to make the system insensitive to changes in the orientation of the reflector as it is moved.

The HeNe beam is reflected by mirror M1, then split at the nonpolarizing beamsplitter, BS. We use a 20 mm cubic 50/50 beam-splitter,¹² but the ratio is not important and a flat plate beamsplitter works equally well. The transmitted beam reflects off M2 and then strikes the cornercube reflector, CC1, which sends the beam back parallel to its original path, with some transverse displacement. The beam reflected from BS travels via M3, M4, and M5 to CC2, where it also is reflected back parallel to its path. Mirror M4 is added to ease alignment as explained later.

The two beams, one from CC1 and the other from CC2, converge at the beamsplitter, producing two output beams. One is used to detect the interferences; the other is used as a tracer, or guide, to align the second laser. The second laser is aligned antiparallel to the beam emitted from the wavemeter and so travels a path exactly the reverse of that traveled by the HeNe beam. The displacement generated by the cornercube reflectors means that no polarizing optics are needed to separate the beams.

The tracer output beam is very convenient, but can destabilize the unknown laser, particularly when used with diode lasers. This problem can be avoided using a Faraday isolator

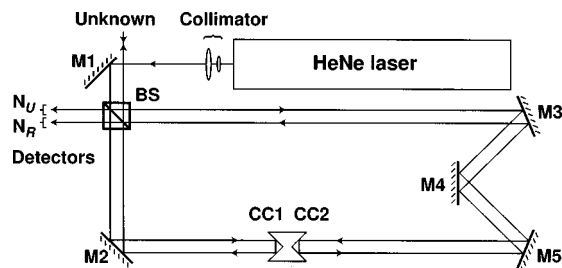


Fig. 2. Wavemeter layout. M1–M5: front-aluminized mirrors, BS: nonpolarizing beamsplitter, plano-convex collimator lenses ($f=4.5, 19$ mm), CC1,2: glass cornercube prisms. The arrows show the beam direction for the reference HeNe laser.

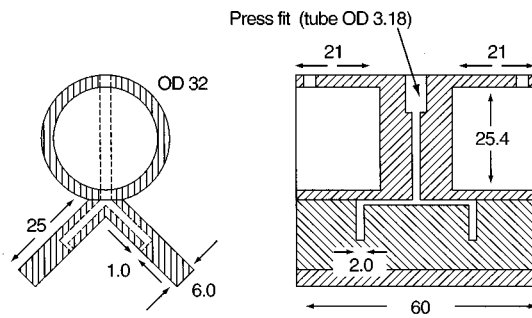


Fig. 3. Wavemeter cart and track, constructed from brass and bearing steel, respectively. The retroreflectors are fixed in place using grub screws with nylon inserts. All dimensions are in millimeters. Note change of scale between cart and track.

on the unknown laser, or by using parallel but nonoverlapping beams in the wavemeter, and indeed several unknown lasers can then be measured simultaneously. With spatially separated beams, air currents and vibrations can cause a difference in the relative optical path lengths of the two beams, but this is generally not significant at an accuracy of 10^{-6} .

Smooth motion of the cornercube reflectors along the track is crucial to the operation of the wavemeter. Transverse motion of the reflectors will produce a displacement in the return beam, such that the beams may no longer overlap at the detector. Hence it is important that the motion of the cornercubes be as laterally stable and as smooth as possible. It is particularly important that any vibrations are so small that they do not add or subtract any interference fringes. In our design, the necessary motion is achieved by mounting the two cornercubes on an air bearing (Fig. 3).

Our air bearing is a simple device that consists of a cart through which flows compressed air. The air is fed into the cart through a soft rubber hose suspended above the device and flows out through four small holes in the bearing face of the cart. The air forms a cushion which supports the cart over a track fabricated from hardened bearing steel. Conventional air tracks have the air directed through small holes all along the track, but this causes variations in the air density and hence index of refraction along the laser path. Reversing this arrangement, so that the air is pumped through small holes in the base of the cart, largely eliminates this problem. The manner in which the cart straddles the track helps to reduce transverse motion.

The wavemeter uses two 25.4 mm glass cornercube prisms, inserted into the cart with the dihedrals (i.e., the junctions between adjacent facets) aligned in parallel. It is then straightforward to avoid laser spots falling on the junctions, which would disturb the interference pattern and increase the risk of false fringe counting. The mirrors are simple front-aluminized plane mirrors and the reference laser is a small (25 mm diameter × 125 mm long) HeNe.¹³ A short HeNe laser was used both to keep the wavemeter compact, and to ensure single-mode operation. The beam produced by the reference laser is collimated with two lenses, of focal lengths 4.5 and 19 mm. This expands the beam by a factor of

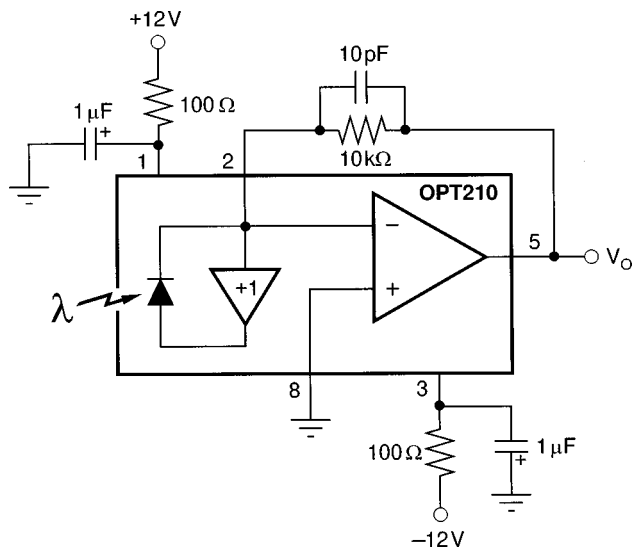


Fig. 4. Monolithic photodiode/amplifier detector configured for 1.6 MHz bandwidth. The OPT210 device includes a bootstrap anode driver (triangle+1) to reduce the effective capacitance of the photodiode to achieve higher bandwidth (Ref. 14).

4 to reduce beam divergence. Note that careful adjustment of the lens separation is required, to obtain flat wavefronts and high-contrast fringes.

The interference fringes can be detected using almost any silicon photodiode, typically reverse biased to reduce response time, and with a transimpedance amplifier to convert current to voltage. We use monolithic photodiode/amplifiers¹⁴ to reduce cost and complexity. These devices directly provide a voltage signal proportional to intensity, with a bandwidth of approximately 1.6 MHz when used as shown (Fig. 4), provided that the incident intensity is below the saturation level of 8 mW cm^{-2} (0.5 mW over the area of the detector). This intensity is easily exceeded and it may be necessary to use some form of attenuation to limit the unknown laser beam intensity. This is best placed just in front of the detector, where the beam quality is no longer important.

The reference and unknown fringes can be counted for a fixed time with conventional frequency counters, and then the unknown wavelength can be calculated from the two counts using Eq. (1). If the counter allows an external reference for determining the counting time, then a single frequency counter can be used and configured to show the wavelength ratio.⁵

It is, however, straightforward to generate a direct wavelength readout. Using Eq. (1), we put the reference wavelength in picometers [$\lambda_R = 632\,823$ (Ref. 15)], so that the unknown wavelength is, in picometers:

$$\lambda_U = \frac{N_R}{N_U} \lambda_R = \frac{N_R}{632\,823} 632\,823 = N_R. \quad (2)$$

That is, as 632 823 fringes are counted from the unknown laser, the number of fringes counted from the HeNe during the same time will be the wavelength of the unknown laser, in picometers. This can be achieved with a counter that starts at 632 823 and counts down on every unknown fringe, while a second counter starts at zero and counts up with every HeNe fringe, until the first counter reaches zero.

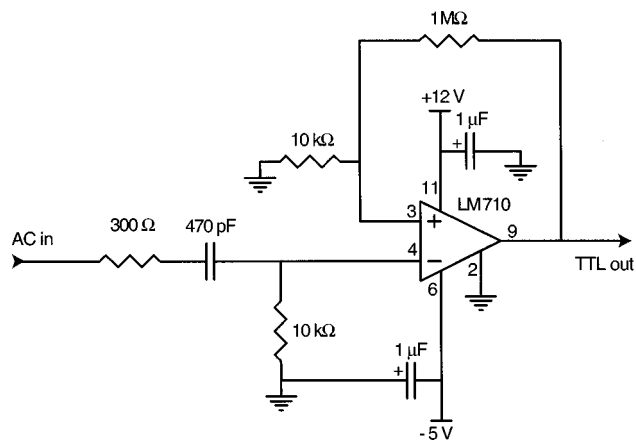


Fig. 5. TTL converter using LM710 comparator.

The sinusoidal signals from each of the detectors are first converted to TTL pulses using comparators (Fig. 5). Figure 6 shows a very low-cost counting circuit which includes both the down-counter and the up-counter with direct picometer display. Counting is initiated by a trigger pulse produced from a slotted optical switch (OC1)¹⁶ at one end of the track. This drives a debounce circuit (74LS221) which then switches a flip-flop (74LS74) on. The flip-flop gates HeNe reference pulses into the display counter, until the binary divider chain, driven by unknown fringes, stops the counting. The final count, i.e., the unknown wavelength in picometers, is then displayed on an LED display. If preferred, a fixed decimal point can be illuminated so that the result is directly read in nanometers. Note that this circuit counts as the cart travels along the track in one direction only and holds that count in the display during the return pass.

III. ALIGNMENT AND OPERATION

It is important that the beams are precisely collinear and parallel to the track so that the interference fringes are generated consistently as the cart moves. We use a straightforward procedure in which we first align the reference laser, and then use the reference as a guide for aligning the unknown laser.

To align the reference, first ensure that the laser beam strikes M1 such that the beam spot does not overlap one of the cornercube dihedrals. Adjust M1 so that the beam passes through the beamsplitter away from the center and then strikes M2. Then rotate the beamsplitter so that the reflected beam travels parallel to the laser and hits M3. Place a beam-stop in this arm of the wavemeter, until M2 is properly aligned. Adjust M2 so that the beam travels parallel to the track, then adjust M1 so that the beam is displaced from the center of the track. This iterative procedure ensures that the return beam does not overlap the incoming beam.

With the cart in place, observe the output beam from the wavemeter and adjust M2 until the position of the spot is completely stable as the cart is moved from one end of the track to the other, thus ensuring that the beams are parallel to the track.

Instead of repeating this process for the other arm of the wavemeter, remove the cart and adjust M3 and M5 until the two beams are counter-propagating. This is best done by ensuring the beam spots on the surfaces of M2 and M5 overlap, but do not move M2, since it is already aligned. Mirror

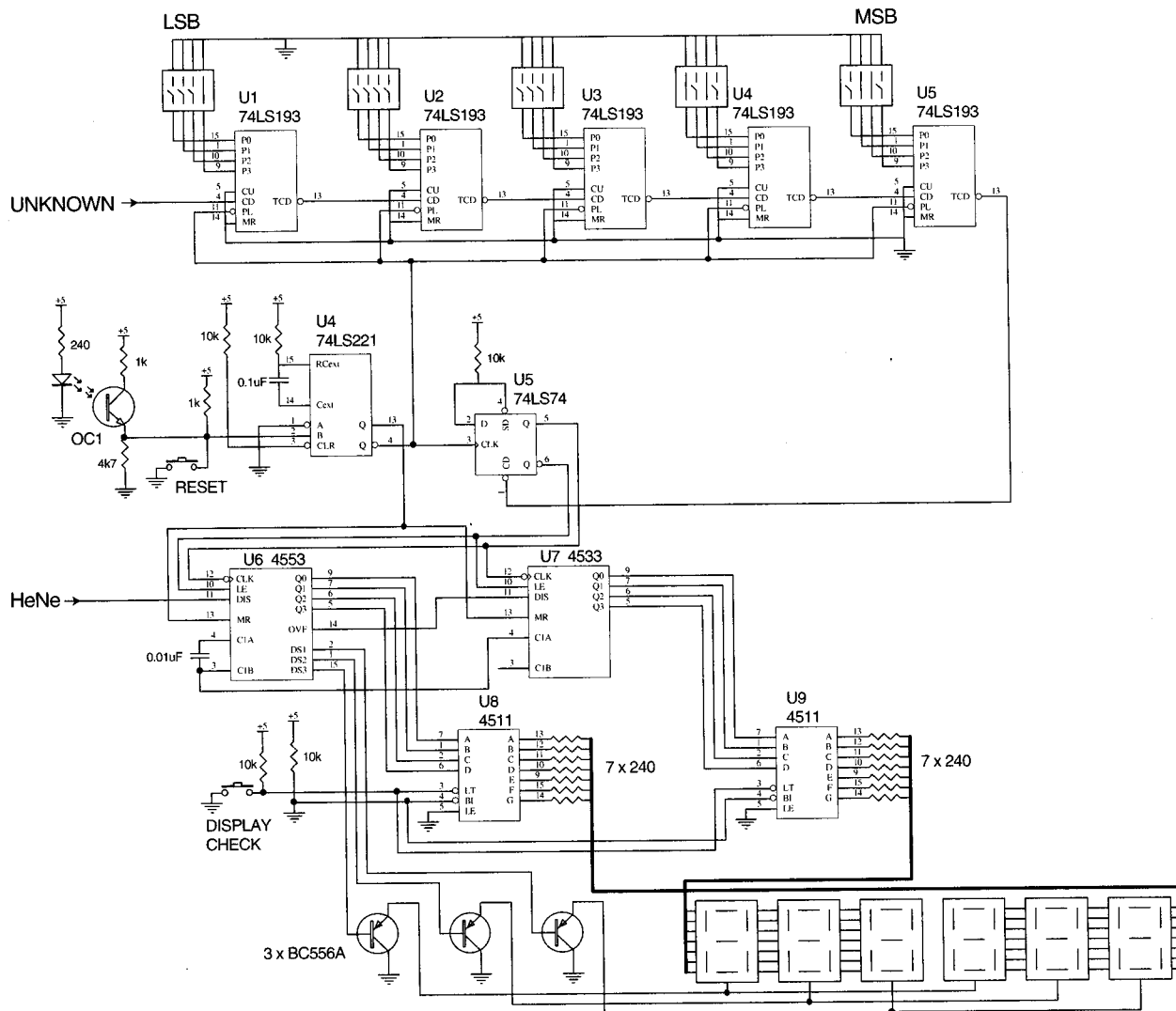


Fig. 6. Wavemeter control and counting circuitry. OC1 is a slotted optical switch (Ref. 16) that detects the presence of the cart at one end of the track. The 74LS193 binary counters are set to count down 632 823 counts so that the wavelength is displayed directly in picometers. The 4511 and 4533 circuits provide a very low cost six-digit counter with seven-segment common cathode display output.

M4 does not need to be adjustable and is present only to correct the geometry so that the beams overlap.

At this stage, interference should be observable by looking at the output beamspot with the air supply pinched off, so that the cart is stationary. Movement of the cart by $\lambda/4$ cycles through one complete interference fringe, so small vibrations in the cart will cause flickering of the output. A detector can then be positioned in the beam and the signal can be seen on an oscilloscope. Small adjustments of the mirrors and focusing of the collimator lenses can then be made so that constant amplitude is maintained as the cart travels the length of the track.

The unknown laser can then be introduced into the system, collinear with the HeNe output tracer beam. This is readily accomplished by reflecting the unknown laser from two mirrors some distance apart and then into the wavemeter. Adjust the mirrors until the beam spots overlap on both mirrors, so that the unknown and output beams are counter-propagating. The unknown beam will travel the exact reverse path through the wavemeter and produce a detection beam slightly dis-

placed from the HeNe, allowing the two detectors to sit side by side and avoiding the need for additional optics to separate the beams.

To make a measurement, the cart must travel the length of the track. We use springs at each end of the track and just give the cart a push when a measurement is required. The smooth, almost frictionless motion of the cart continues unaided for several minutes, allowing many measurements before the cart stops. If the wavelength must be monitored constantly, then solenoids can be used to kick the cart at one or both ends of the track.¹⁷

The ability of the wavemeter to accurately determine the wavelength was tested by taking 100 measurements of a 780 nm diode laser, locked to the $5S_{1/2} \rightarrow 5P_{3/2}$ transition in rubidium. The results shown in Fig. 7 indicate that there is a variation of 1 in the last digit. The standard deviation in these results is less than 0.001 nm, which is at the limit of the counting resolution of the device. The absolute accuracy, however, is limited by systematic errors.

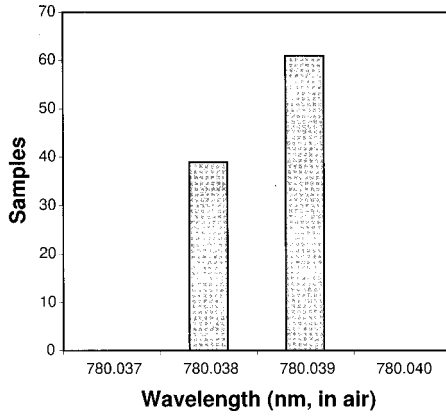


Fig. 7. Distribution of wavemeter measurements of a 780 nm diode laser locked to the $5S_{1/2} \rightarrow 5P_{3/2}$ transition in rubidium, for 100 samples.

IV. ACCURACY LIMITATIONS

The accuracy of Michelson wavemeters has been discussed at length by several authors.^{3,7} We briefly review the uncertainties¹⁸ and show that our device is fundamentally limited by the number of fringes counted and the stability of our HeNe reference.

The uncertainty includes contributions from wavefront curvature and misalignment of the beam from mirror adjustment, which produce errors in the number of fringes counted. The reference HeNe laser frequency is defined only to the width of the Doppler spread in the gain curve, and also depends on the blend of Ne isotopes used in the laser tube. Finally, the counting resolution also limits the accuracy. These uncertainties can be added in quadrature to produce an estimate for the uncertainty of the measurement:

$$\left(\frac{\Delta\lambda}{\lambda}\right)^2 = \left(\frac{\Delta\lambda_{\text{WC}}}{\lambda}\right)^2 + \left(\frac{\Delta\lambda_{\text{align}}}{\lambda}\right)^2 + \left(\frac{\Delta\lambda_{\text{HeNe}}}{\lambda}\right)^2 + \left(\frac{\Delta\lambda_{\text{count}}}{\lambda}\right)^2, \quad (3)$$

where $\Delta\lambda_{\text{WC}}$, $\Delta\lambda_{\text{align}}$, $\Delta\lambda_{\text{HeNe}}$, and $\Delta\lambda_{\text{count}}$ are the uncertainties due to wavefront curvature, beam misalignment, HeNe wavelength, and counting resolution.

Wavefront curvature in the laser beams will result in counting errors due to diffraction effects.⁷ The magnitude of the uncertainty can be estimated from simple diffraction theory, and is given by

$$\left(\frac{\Delta\lambda_{\text{WC}}}{\lambda}\right)^2 = \frac{\lambda^2}{4\pi^2\omega_0^2} = \frac{\Delta\theta^2}{4}, \quad (4)$$

where ω_0 is the beam waist diameter and $\Delta\theta$ is the divergence of the beam. The divergence of the diode laser is 0.17 mrad and that of the HeNe is 0.25 mrad which gives

$$\left(\frac{\Delta\lambda_{\text{WC}}}{\lambda}\right)_{\text{HeNe}} = 1.56 \times 10^{-8}, \quad (5)$$

$$\left(\frac{\Delta\lambda_{\text{WC}}}{\lambda}\right)_{\text{DL}} = 6.94 \times 10^{-9}. \quad (6)$$

Relative misalignment of the reference and unknown beams will produce counting errors since the lengths traveled by the two beams will differ. This is a simple cosine error, which is, for small angles,

$$\left(\frac{\Delta\lambda_{\text{align}}}{\lambda}\right) = \left(\frac{\Delta L}{L}\right) = \frac{1}{2} \left(\frac{\Delta x}{L}\right)^2, \quad (7)$$

where $\Delta x/L$ is the relative angular displacement. The optical path length is $L = 0.494$ m, and taking an extreme relative displacement over that distance of $\Delta x = 0.5$ mm, the beam misalignment uncertainty is $(\Delta L/L)_{\text{align}} = 5.1 \times 10^{-7}$. In practice, obtaining fringes of constant amplitude over the length of the track ensures much better alignment.

The HeNe laser wavelength is uncertain due to the ≈ 1.5 GHz Doppler width of the Ne emission line, and to the unknown Ne isotope mixture used in the tube. The Doppler width corresponds to a wavelength uncertainty of 2 pm; that is, $\Delta\lambda_{\text{Doppler}}/\lambda = 3.2 \times 10^{-6}$. The unknown isotopic mixture gives an uncertainty of approximately 1 pm.¹⁹ Both uncertainties can be minimized by locking the HeNe laser to an I_2 absorption line.¹⁹ The larger Doppler uncertainty can more easily be reduced by simply stabilizing the HeNe, in particular by controlling the cavity temperature to obtain equal intensities of two operating longitudinal modes with orthogonal polarization.¹⁵

The limited number of fringes counted during the measurement determines the ultimate accuracy for our device. In measuring a laser at $\lambda_U = 780$ nm, 632 823 fringes are counted from the unknown laser, and $780\,000 \pm 1$ fringes are counted from the HeNe. The uncertainty due to fringe counting is then

$$\left(\frac{\Delta\lambda_{\text{count}}}{\lambda}\right) = \frac{1}{780\,000} = 1.28 \times 10^{-6}. \quad (8)$$

Summing the uncertainties in quadrature [Eq. (3)] we see that the HeNe wavelength uncertainty and the counting error far outweigh all others. The final relative accuracy is $(\Delta\lambda/\lambda) = 3.8 \times 10^{-6}$, which, when applied to the data obtained earlier, gives a wavelength measurement of $\lambda = 780.039 \pm 0.003$ nm, in air. The wavelength uncertainty corresponds to a frequency uncertainty of ≈ 1.5 GHz, small enough to tune the diode laser to within a Doppler-broadened atomic resonance.

These measurements are for the unknown wavelength in air. If the vacuum wavelength is required, then the vacuum wavelength for the reference laser can be substituted into Eq. (1), but there is also a small correction for the dispersion of air. The vacuum wavelength λ_{U_0} and frequency ν_U of the unknown laser are

$$\lambda_{U_0} = \frac{N_R}{N_U} \lambda_{R0} \left(\frac{n_U}{n_R}\right), \quad (9)$$

$$\nu_U = \frac{N_U}{N_R} \nu_R \left(\frac{n_R}{n_U}\right), \quad (10)$$

where N_U and N_R are the number of fringes counted from the unknown and HeNe lasers, ν_R is the frequency of the HeNe reference (473.612 THz²⁰), and λ_{R0} is the vacuum wavelength (632 991 pm). n_U and n_R are the refractive indices of air at the known and unknown wavelengths. For 780 nm this ratio²¹ gives a correction of one count; that is, the

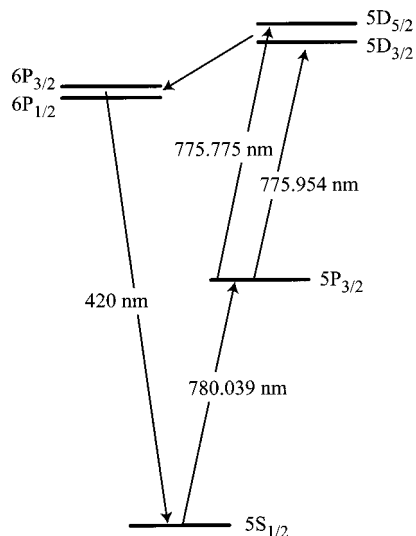


Fig. 8. Energy level diagram for ^{85}Rb , omitting the hyperfine levels. Wavelengths of the 776 and 780 nm transitions are as measured with the wavemeter, in air.

vacuum wavelength is 1 pm shorter than calculated without the correction for dispersion.

V. TWO-STEP EXCITATION

As a demonstration of the wavemeter, we have used it to study two-step excitation. In this experiment, two lasers were counter-propagating through a Rb vapor cell. One laser was tuned to the $5^2\text{S}_{1/2}(F=3) \rightarrow 5^2\text{P}_{3/2}(F=4)$ resonant transition in Rb at 780 nm, while the second laser was tuned to either the $5^2\text{P}_{3/2} \rightarrow 5^2\text{D}_{3/2}$ or the $5^2\text{P}_{3/2} \rightarrow 5^2\text{D}_{5/2}$ transition, at 776 nm (Fig. 8).

In addition to decay through the 5^2P state, the selection rules allow for decay through the 6^2P states, from where they can decay directly to the 5^2S ground state, emitting photons at 420 nm.

Counter-propagating lasers were used to select atoms with the same velocity component along the laser beams. Atoms excited to one of the 5^2P hyperfine levels by the first laser have a velocity component along the laser defined by the laser detuning from resonance. To excite these atoms to a given 5^2D hyperfine level, the second laser must be detuned by exactly the same amount, but with opposite sign. Thus counter-propagating lasers select a narrow velocity group from the broad (≈ 500 MHz) Maxwellian velocity distribution in the vapor cell, and both lasers must be tuned very precisely to their respective atomic resonances before blue fluorescence can be observed.

A photomultiplier tube and lens were positioned perpendicular to the laser beams to observe the blue fluorescence. A 420 nm interference filter was used to exclude the spontaneous decay at 780 and 776 nm.

The first laser was tuned to the $5^2\text{S}_{1/2}(F=3) \rightarrow 5^2\text{P}_{3/2}(F=4)$ transition using the wavemeter, and then locked using saturated absorption locking in a separate vapor cell.²² The second laser was tuned close to the $5^2\text{P}_{3/2} \rightarrow 5^2\text{D}_{3/2}$ transitions at 776 nm, again using the wavemeter. The laser was then smoothly scanned through several GHz until blue light at 420 nm was observed. The laser was carefully tuned to the

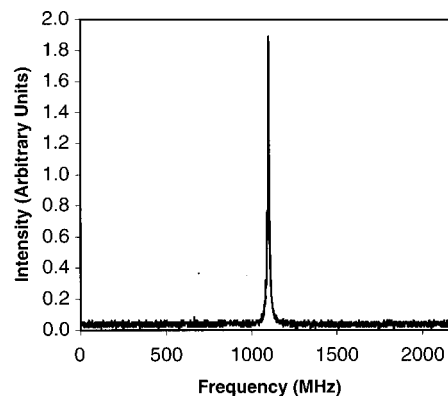


Fig. 9. Intensity of blue fluorescence emitted as the 776 nm laser was scanned through the $5^2\text{P}_{3/2} \rightarrow 5^2\text{D}_{3/2}$ transition. The peak includes two unresolved hyperfine levels ($F=3,4$). The frequency span was calibrated using an optical spectrum analyzer with 300 MHz free spectral range.

peak emission, and the wavemeter used to measure the wavelength: 775.775 ± 0.003 nm (in air). Finally, the 776 nm laser was scanned smoothly through the resonance and the emission recorded, as shown in Fig. 9.

The 776 nm laser was also tuned to the $5^2\text{D}_{5/2}$ transition, which is lower in frequency by about 90 GHz. Using the wavemeter, we obtained a value of 775.954 ± 0.003 nm, in air.

The observation of the blue light emitted from the vapor cell is indication that the two-step process has occurred. This sort of experiment requires two lasers tuned very precisely to atomic transitions, which is only feasible using a wavemeter to monitor the wavelength in real time with a high accuracy.

VI. FURTHER IMPROVEMENTS

The precision and repeatability of the wavemeter are clearly within one fringe count, as shown by Fig. 7. The accuracy is somewhat poorer than the resolution, largely due to the Doppler width of the HeNe reference gain curve. Once the laser has reached an equilibrium temperature, it prefers to oscillate at close to the peak of this gain curve, and its frequency uncertainty drops by a factor of 5 to 10, hence the repeatability is much better than might otherwise be expected. As mentioned, the uncertainty can be reduced substantially with the addition of a simple locking circuit,¹⁵ such that the accuracy is limited by counting error. The counting error can be reduced by increasing the track length, or by fringe interpolation or fringe multiplication.^{4,9,10} With such modifications, the accuracy can exceed the best commercial devices.

VII. CONCLUSION

This very compact wavemeter provides sufficient accuracy to tune a laser to a Doppler-broadened atomic resonance, yet it is simple and cheap enough that it can be incorporated into an undergraduate laboratory in optical or atomic physics. The device has a relative uncertainty of 3.8×10^{-6} overall, typically 3 pm, and the precision to measure relative wavelengths to within 1 least significant digit, typically 1 pm. A panel readout showing the unknown wavelength is updated in real time, making the device ideal for monitoring a tunable laser, either as it is adjusted or during its use. This wavemeter is currently in regular use in our research laboratory. The

size of the device also makes it possible to move the wavemeter quite readily, and the tracer output allows configuration for new measurements with only a few minutes of external mirror alignment.

ACKNOWLEDGMENTS

We gratefully acknowledge the support of the Australian Research Council, and the Australian Postgraduate Research Awards scheme (PJF, MRW).

- ¹K. B. MacAdam, A. Steinbach, and C. Weiman, "A narrow-band tunable diode laser system with grating feedback, and a saturated absorption spectrometer for Cs and Rb," *Am. J. Phys.* **60**, 1098–1111 (1992); K. G. Libbrecht, R. A. Boyd, P. A. Williams, T. L. Gustavson, and D. K. Kim, "Teaching physics with 670 nm diode lasers—construction of stabilized lasers and lithium cells," *Am. J. Phys.* **63**, 1–8 (1995); A. S. Arnold, J. S. Wilson, and M. G. Boshier, "A simple extended-cavity laser," *Rev. Sci. Instrum.* **69**, 1236–1239 (1998).
- ²J. J. Snyder, "Algorithm for fast digital analysis of interference signals," *Appl. Opt.* **19**, 1223–1225 (1980).
- ³R. Castell, W. Demtröder, A. Fischer, R. Kullmer, H. Weickenmeier, and K. Wickert, "The accuracy of laser wavelength meters," *Appl. Opt.* **38**, 1–10 (1985).
- ⁴J. L. Hall and S. A. Lee, "Interferometric real-time display of cw dye laser wavelength with sub-Doppler accuracy," *Appl. Phys. Lett.* **29**, 367–369 (1976).
- ⁵F. V. Kowalski, R. T. Hawkins, and A. L. Schawlow, "Digital wavemeter for cw lasers," *J. Opt. Soc. Am.* **66**, 965–966 (1976).
- ⁶J. Ishikawa, N. Ito, and K. Tanaka, "Accurate wavelength meter for cw lasers," *Appl. Opt.* **25**, 639–643 (1986).
- ⁷J.-P. Monchalain, M. J. Kelly, J. E. Thomas, N. A. Kurnit, A. Szöke, F. Zernike, P. H. Lee, and A. Javan, "Accurate laser wavelength measurement with a precision two-beam scanning Michelson interferometer," *Appl. Opt.* **20**, 736–757 (1981).
- ⁸X. Hui-Rong, S. V. Benson, and T. W. Hänsch, "A 'toy-train' wavemeter," *Laser Focus* **17**, 54–58 (1981).
- ⁹F. V. Kowalski, R. E. Teets, W. Demtröder, and A. L. Schawlow, "An improved wavemeter for cw lasers," *J. Opt. Soc. Am.* **68**, 1611–1613 (1978).
- ¹⁰There have been many papers with various improvements to the basic wavemeter design, including: J. Cachena, C. Man, P. Cerez, A. Brillat, F. Stoeckel, A. Jourdan, and F. Hartmann, "Description and accuracy tests of an improved lambda-meter," *Rev. Phys. Appl.* **14**, 685–688 (1979); S. J. Bennett and P. Gill, "A digital interferometer for wavelength measurement," *J. Phys. E* **13**, 174–177 (1980); H. K. Carter, C. R. Bingham, D. J. Pegg, M. L. Gaillard, E. F. Zganjar, and P. M. Griffin, "A precise real-time wavemeter," *Nucl. Instrum. Methods Phys. Res.* **202**, 361–364 (1982); A. Kahane, M. S. O'Sullivan, N. M. Sanford, and B. P. Stoicheff, "Vernier fringe-counting device for laser wavelength measurements," *Rev. Sci. Instrum.* **54**, 1138–1142 (1983); A. Bränberg and P. Nylén, "Vacuum-operated digital wavelength meter," *ibid.* **56**, 211–213 (1985); J. Kowalski, R. Neumann, S. Noehte, R. Schwarzwald, H. Suhr, and G. Zu Putlitz, "An automatic Michelson interferometer with fringe dropout correction," *Opt. Commun.* **53**, 141–146 (1985); M. Braun, J. Maier, and H. Liening, "A high precision compact Michelson-Sagnac wavemeter," *J. Phys. E* **20**, 1247–1249 (1987); S. M. Jaffee and W. M. Yen, "A precision drive for a Michelson wavemeter," *Rev. Sci. Instrum.* **64**, 1459–1462 (1993).
- ¹¹A packaged version of this wavemeter, with engineering refinements and precision options reaching a part in 10^9 , is available from R. E. Drullinger, NIST Time and Frequency Division, Boulder, CO.
- ¹²The cornercubes and beamsplitter are from Edmund Scientific, stock numbers M43,297 and M32,504. Note: certain commercial equipment, instruments, or materials are identified in this paper in order to adequately specify the experimental procedure. Such identification does not imply recommendation or endorsement by the National Institute of Standards and Technology, nor does it imply that the materials or equipment identified are necessarily the best available for the purpose.
- ¹³MWK Industries, Catalog No. DCK2.
- ¹⁴Burr-Brown Corporation, OPT-210.
- ¹⁵R. Balhorn, H. Kunzmann, and F. Lebowsky, "Frequency Stabilization of Internal-Mirror Helium-Neon Lasers," *Appl. Opt.* **11**, 742–744 (1972); T. M. Niebauer, J. E. Faller, H. M. Godwin, J. L. Hall, and R. L. Barger, "Frequency stability measurements on polarization-stabilized He-Ne lasers," *Appl. Opt.* **27**, 1285–1289 (1988).
- ¹⁶Omron EE-SG3.
- ¹⁷B. W. Petley and K. Morris, "A simple CW laser digital wavemeter," *Opt. Quantum Electron.* **10**, 277–278 (1978).
- ¹⁸Our uncertainties are one standard deviation.
- ¹⁹W. G. Schweitzer, Jr., E. G. Kessler, Jr., R. D. Deslattes, H. P. Layer, and J. R. Whetstone, "Description, Performance, and Wavelengths of Iodine Stabilized Lasers," *Appl. Opt.* **12**, 2927–2938 (1973).
- ²⁰D. A. Jennings, C. R. Pollock, F. R. Petersen, R. E. Drullinger, K. M. Evenson, J. S. Wells, J. L. Hall, and H. P. Layer, "Direct frequency measurement of the I₂-stabilized He-Ne 473 THz (633 nm) laser," *Opt. Lett.* **8**, 136–138 (1983).
- ²¹B. Edlen, "The Refractive Index of Air," *Metrologia* **2**, 71–80 (1966); J. C. Owens, "Optical Refractive Index of Air: Dependence on Pressure, Temperature and Composition," *Appl. Opt.* **6**, 51–59 (1967).
- ²²T. P. Dinneen, C. D. Wallace, and P. L. Gould, "Narrow linewidth, highly stable, tunable diode laser system," *Opt. Commun.* **92**, 277–282 (1992).

CONVICTIONS

It is well to think of physics as comprising two phases, knowledge of facts and knowledge of ideas. By knowledge of ideas I mean the kind of mental adaptation which makes the student a critical appraiser of that which he learns. In certain other branches of knowledge, in the social sciences, for example, and even in the arts, the junior student has frequently strong convictions concerning what he learns. He may find himself wrong in those convictions, but I believe it is better to have wrong convictions than no convictions at all.

W. F. G. Swann, "The Teaching of Physics," *Am. J. Phys.* **19** (3), 182–187 (1951).